

The Application of Decomposition to the Large Scale Synthesis/Design Optimization of Aircraft Energy Systems

Jules R. MUÑOZ[†] and Michael R. von SPAKOVSKY
Energy Management Institute
Department of Mechanical Engineering
Virginia Polytechnic Institute and State University
Blacksburg, VA 24061
Fax: (540) 231-9100
E-mail: munozjr@utrc.utc.com or vonspako@vt.edu

Abstract

An application of a decomposition approach for large-scale optimization (i.e., the Iterative Local-Global Optimization (ILGO) approach) developed by Muñoz and von Spakovsky (2001) is presented. The synthesis / design optimization of a turbofan engine coupled to an environmental control system for a military aircraft was carried out. The problem was solved for a given mission (i.e. a load / environmental profile) composed of fifteen segments. The number of decision (independent) variables both discrete and continuous for this highly non-linear optimization problem was one hundred fifty-three. Both the thermodynamic and physical (weight and volume) simulations were carried out using state-of-the art tools. Three objective functions were investigated: take-off gross weight, mission fuel consumption and total cost, and no observable differences were found in the final results. In addition to the mathematical foundations for global convergence presented in Muñoz and von Spakovsky (2000b, 2001), convergence was validated numerically by solving the entire mixed-integer non-linear programming (MINLP) problem without decomposition using a subset of the independent variables. The constant value of the shadow prices (or linear behavior of the Optimum Response Surface – OSR) played a major role in global convergence of the ILGO approach.

Key words: optimization, decomposition, aircraft synthesis / design, multi-disciplinary design optimization (MDO), thermoeconomics

1. Introduction

The integration challenges and the highly dynamic characteristics of aircraft systems have produced a growing interest in Second Law Analysis and Thermoeconomics by both the aerospace industry and researchers. The interdependency of subsystems creates the need for detailed analyses of the energy and exergy exchanges at the operational level and the integration of components and subsystems to accomplish the system objectives at the synthesis / design level.

To achieve the performance and affordability requirements normally imposed upon an aircraft design, it is necessary to create thermodynamic, physical (weight and size), and cost models for the entire system as a function of the geometric, flow, and technological variables involved. The high fidelity required by the simulations, the tight integration and the highly dynamic nature of the operation and environmental conditions pose a great challenge in terms of the synthesis/design optimization of the system. These characteristics make the problem ideally suited for the application of a

[†] Now at United Technologies Research Center, East Hartford, CT.

decomposition approach for large-scale optimization such as the Iterative Local-Global Optimization (ILGO) approach presented in Muñoz and von Spakovsky (2001).

The application presented in this paper is the integrated synthesis/design optimization of two sub-systems, which are part of an advanced military aircraft. The problem to be solved in an integrated fashion is the optimal conceptual design of a low-bypass turbofan engine with afterburning (Propulsion Sub-system - PS) and the synthesis and design optimization of an air-cycle Environmental Control System (ECS).

The PS provides the necessary thrust for the vehicle to carry out the desired mission. The mission¹ is the set of conditions under which the aircraft must be synthesized / designed. In this paper, the mission defined by the Request for Proposal (RFP) for an Air-to-Air Fighter (AAF) given by Mattingly et al. (1987) is used. The mission has 15 different phases or legs as shown in Figure 1. In addition to providing the required rates of climb and acceleration and overcoming the aircraft's drag, the PS must provide the power required to operate all the remaining sub-systems, including the ECS.

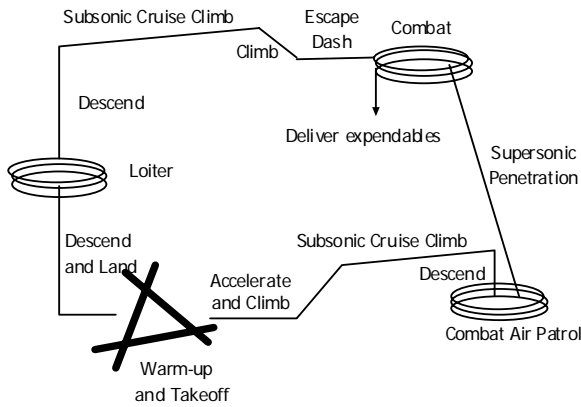


Figure 1. Mission profile by phase or leg (Mattingly et al., 1987).

The ECS provides the cooling necessary to dissipate the heat generated in the aircraft. A set of cooling requirements has been added to the mission according to the design specifications given by Muñoz and von Spakovsky (1999).

An energy balance along with the traditional aircraft lift and drag coefficients can be

¹ The mission is equivalent to the load profile and set of environmental conditions in a stationary application.

manipulated to produce the thrust equation for the i_{th} leg, namely

$$T_i = \alpha T_{SL} = \frac{\beta_i W_{TO}}{V_i} \frac{d}{dt} \left(h_i + \frac{V_i^2}{2g} \right) + q_i S \left[K_1 \left(\frac{n_i \beta_i W_{TO}}{q_i S} \right)^2 + C_{D0} + \frac{D_{ECS_i}}{q_i S} \right] \quad (1)$$

where C_{D0} and K_1 are a function of the Mach number and correspond to high performance aircraft (Muñoz and von Spakovsky, 2000c). In the above equation, n is the load factor, which is equal to the number of g 's perpendicular to the direction of the velocity, T_{SL} is the thrust at sea level take-off, W_{TO} is the gross take-off weight, and β_i is the fraction of the take-off weight for leg i . The only additional drag, R , considered is the momentum drag created by the ECS (i.e. $R = D_{ECS}$). The velocity (V) and the rates of climb (dh/dt) and acceleration (dV/dt) are directly or indirectly given by the mission specifications. The drag created by the ECS is also leg-dependent as will be discussed below. The take-off gross weight (W_{TO}) is given by

$$W_{TO} = W_{STR} + W_{PS} + W_{ECS} + W_{FUEL} + W_{PPAY} + W_{EPAY} \quad (2)$$

where W_{STR} is the weight of the structures, which in this paper refers to all sub-systems present in the aircraft (wing, fuselage, hydraulics, power distribution, etc.) with the exception of the ECS, the weapons and the PS. W_{PS} is the weight of the engine (propulsion sub-system), W_{ECS} is the weight of the ECS, W_{FUEL} is the weight of fuel necessary to carry out the mission, W_{PPAY} is the weight of the permanent payload (crew, equipment) and W_{EPAY} is the expendable payload (ammunition and missiles).

An analysis of the constraints of the RFP will show a functional relationship between the minimum thrust-to-weight ratio or thrust loading at sea-level takeoff (T_{SL}/W_{TO}) and wing loading at take-off (W_{TO}/S). The construction of the resulting constraint diagram is beyond the scope of this paper (the interested reader may consult the aircraft performance and design book by Nicolai (1975)). Based on the complete constraint diagram for the AAF given by Mattingly et al. (1987), the following values for the thrust and wing loading are selected:

$$\frac{T_{SL}}{W_{TO}} = 1.20 \quad (3)$$

$$\text{and } \frac{T_{SL}}{S} = 3065 \text{ N/m}^2 \quad (4)$$

Equations (1) through (4) hint at the tight integration issues associated with the synthesis/design of an aircraft. The synthesis/design and operation of any given sub-system is highly influenced by and in turn influences the synthesis/design and operation of all the others. Take the case of the ECS, for example. The ECS' weight and energy and extra thrust requirements affect the required total thrust which leads to higher fuel consumption and higher take-off gross weight. Equation (3) clearly shows that an increase in W_{TO} is associated with higher thrust, which in turn affects the size of the PS. The size (weight) of the structures is also affected as indicated by equation (4).

Based on the above, one can conclude that, in general, when any sub-system is installed in an aircraft, additional fuel (with the consequent effect on system weight) is required to

- provide the additional thrust associated with carrying the increased system mass
- overcome any additional drag, which may result from installing the subsystem in the aircraft
- carry the quantity of fuel required for the previous items.
- produce the power that some sub-systems may require. Power extractions from the PS cause increased fuel consumption and the associated larger weight discussed above.

Let us now turn our attention to the calculation of each one of the terms in the weight equation (2). The fuel weight is calculated based on engine performance and mission requirements and depends on the system synthesis / design and mission requirements. The weight of the ECS and the PS result from the sub-system optimization problems. The weight of the structures depends on a number of synthesis/design considerations: materials used, aerodynamic performance, durability, strength and stability among many others.

The synthesis/design of the structures is beyond the scope of this paper. Here we consider the weight of the structures to correspond to values in agreement with existing design practices. To this end we obtained correlations of empty weight (structures plus PS plus ECS) and PS weight versus W_{TO} using data found in the literature (Jane's All the World's Aircraft 1999-2000). The ECS weight was subtracted from the empty weight as indicated by Muñoz and von Spakovsky (2000c).

The fuel weight in equation (2) is a complex function of the thermodynamic performance of the engine, the mission requirements, the technology used and some stability considerations. In general, it is given by

$$W_{FUEL} = g \sum_{mission} \dot{m}_i \Delta t_i = g \sum_{mission} TSFC_i \cdot T_i \cdot \Delta t_i \quad (5)$$

where the rate of fuel consumption has been written in terms of the thrust specific fuel consumption ($TSFC_i$) at leg i .

Equation (5), however, is fairly inconvenient due to the fact that the specifications of each of the mission legs are given in terms of different parameters. Some of the legs have specified range, others specified duration, while still others have specific maneuvers to be carried out. In addition, the duration of some of the legs changes as the decision variables are varied. Therefore, it is useful to employ a transformation, which puts all mission segments under a unified measure. Fuel consumed in each leg written in terms of the weight ratio is such a measure. The ratio of the final to the initial weight for leg i is defined as

$$\pi_i = W_{final} / W_{initial} \quad (6)$$

In order to proceed with the calculation of the weight ratios, consider the rate at which aircraft weight diminishes due to the consumption of fuel, namely

$$\frac{dW}{W} = -TSFC \frac{T}{W} dt = -TSFC \frac{T}{W} \frac{ds}{V} \quad (7)$$

Equation (7) represents the weight-time and weight-velocity transformation that is used to unify the different requirements of the mission. The integration of equation (7) is done by breaking each mission segment (phase or leg) into several (typically 5) intervals. The flight and operating conditions for each sub-segment are assumed to be constant at some representative value so that the integration can be accomplished explicitly. It was found that in most cases, five intervals are sufficient to ensure excellent accuracy. The resulting weight ratio relations are given in detail by Muñoz and von Spakovsky (2000c).

There is a special case, however, which deviates from the above calculations and corresponds to the mission instant when the expendable payload is delivered. If it is assumed that the delivery is done at some point j in the mission then

$$\frac{W_j - W_{EPAY}}{W_j} = 1 - \frac{W_{EPAY}}{W_j} \quad (8)$$

With equation (8) and the weight ratios and after some manipulation, the fuel consumption can be written as

$$W_{FUEL} = W_{TO} \left(1 - \prod_{i=1}^n \pi_i\right) - W_{EPAY} \left(1 - \prod_{i=j}^n \pi_i\right) \quad (9)$$

where n is the number of legs being considered.

The weight fractions depend on the design of the PS and the other sub-systems, the thrust required, the afterburner setting and power requirements of the other sub-systems, ambient conditions, and a number of other factors.

2. Problem Definition

2.1 PS Models and decision variables

The PS has eighteen components as indicated in *Figure 2*. This sub-system is a low-bypass turbofan engine with afterburning. The on and off-design behavior of the engine is simulated using a modern performance code developed by an engine manufacturer for modeling any type of aircraft engine system. The model of the engine uses typical component maps (e.g., compressor, fan hub, fan tip, turbine, burner, and compressor maps) and functional relationships and numerical constants that modify the maps to make the simulation as realistic as possible. The weight and dimensions of the PS are calculated using the computer code Weight Analysis of Turbine Engines (WATE) (WATE User's Guide, 2000). WATE was originally developed by the Boeing Military Aircraft Company in 1979 and improved by NASA and the McDonnell Douglas Corporation. The code is based on analytical and dimensional calculations (the primary method is to calculate material volume and then multiply by density). A complete description of the thermodynamic and physical models is given by Muñoz and von Spakovsky (2000c). The cost model uses equations for estimating development and production costs for military turbojet and turbofan engines as a function of the vehicle's Mach number, turbine inlet temperature, and T_{SL} . The model was obtained by applying regression analysis to available data. Further details of the cost model are found in Muñoz (2000).

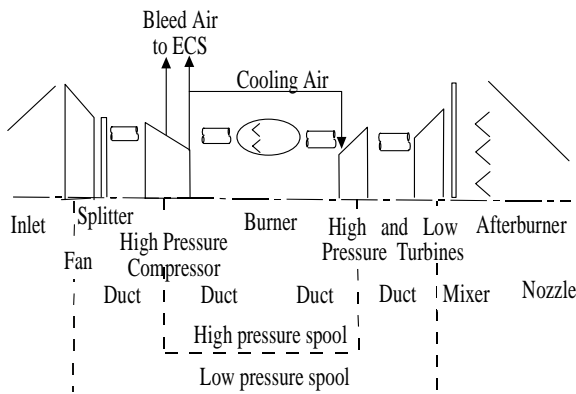
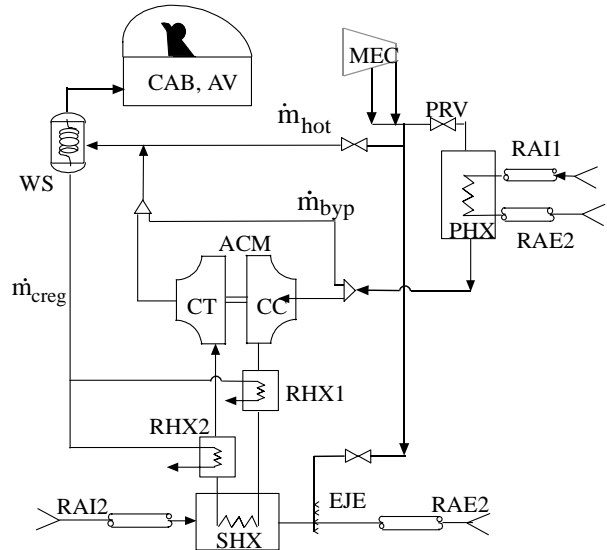


Figure 2. Turbofan engine components of the propulsion sub-system (PS).



WS	Water separator	AV	Avionics
MEC	Main Engine Compressor	RAI1 RAI2	First and Second Ram Air Inlets
PRV	Pressure Regulating Valve	RAE1 RAE2	First and Second Ram Air Exits
CC CT	Centrifugal Compressor and Turbine	\dot{m}_{creg}	Regenerative Heat Exchanger Cold air flow rate
CAB	Cabin	EJE	Ejector
RHX1 RHX2	1st and 2nd Regenerative HX	ACM	Air Cycle Machine
PHX SHX	Primary and Secondary Heat Exchangers	\dot{m}_{hot} \dot{m}_{byp}	Hot bleed air Bypass air

Figure 3. Environmental Control Sub-system (ECS) and components.

2.2 ECS Models and Decision Variables

The ECS provides the cooling necessary to dissipate the heat generated by the multiple heat sources in an aircraft. The ECS being considered is a bootstrap subsystem as shown in *Figure 3*. The ECS thermodynamic model was developed using performance maps of typical components. The size (volume and mass) is calculated using the geometry of each component. Correlations for the cost of each component as a function of the geometry were developed using information from various sources. A detailed description of the models is given in Muñoz and von Spakovsky (1999, 2000a,c).

The synthesis/design and operational independent (decision) variables for the ECS are given in TABLE II. The range of the independent variables is based on existing designs.

The design and operational independent (decision) variables for the PS are given in TABLE I. Their ranges were selected based on existing engines with the proper thrust class. All of the components in the PS use current (year 2000) technology. Other important design

parameters, which are fixed during the optimization, are listed in Muñoz and von Spakovsky (2000c).

TABLE I. PS DECISION VARIABLES AND CONSTRAINTS.

Component	Design Decision Variables		Constraints
Fan	α	Fan bypass ratio	$0.3 \leq \alpha \leq 0.6$
	PR_{fan}	Fan design pressure ratio (tip and hub)	$3.0 \leq PR_{fan} \leq 5.0$
Compressor	PR_{hpc}	High pressure compressor design pressure ratio	$4.0 \leq PR_{hpc} \leq 8.0$
Turbine	PR_{hpt}	High pressure turbine design pressure ratio	$1.8 \leq PR_{hpt} \leq 3.0$
	PR_{lpt}	Low pressure turbine design pressure ratio	$1.8 \leq PR_{lpt} \leq 3.0$
Mixer	M_{mixer}	Mixer Mach number	$M_{mixer} = 0.4$
Operational Decision Variables			
Compressor	BP_{low}	Low pressure bleed port ²	$BP_{low} = 0, 1$
	BP_{high}	High pressure bleed port ²	$BP_{high} = 0, 1$
Turbine	T_{it}	Turbine inlet temperature	$T_{it} \leq 1778 \text{ K}$
Dependent Variables			
Afterburner	T_{aft}	Afterburner temperature ³	$T_{aft} \leq 2000 \text{ K}$
Fan	ϕ_{hub}	Fan (hub) % stall margin ³	$\phi_{hub} > 10$
	ϕ_{tip}	Fan (tip) % stall margin ²	$\phi_{tip} > 10$
Fan and compressor	PR_{cp}	Overall pressure ratio	$17 \leq PR_{cp} \leq 32$
Compressor	ϕ_{hpc}	Compressor % stall margin ²	$\phi_{hpc} > 10$
	N/A	Bleed port selection ²	$BP_{low} + BP_{high} = 1$

3. Optimization Problem Definitions

3.1 Gross take-off weight problem definition⁴

The first optimization problem formulated is that for the conceptual design optimization of a turbofan engine with afterburner (PS) integrated with the synthesis / design optimization of the ECS for a military AAF using the mission given in Figure 1 and gross take-off weight as the figure of merit. Thus, the problem is to

Minimize

$$W_{TO} = W_{STR} + W_{PS} + W_{ECS} + W_{FUEL} + W_{PPAY} + W_{EPAY} \quad (10)$$

$$\text{w.r.t. } \{\bar{X}_{PS}, \bar{Y}_{PS}\}; \{\bar{X}_{ECS}, \bar{Y}_{ECS}\}$$

subject to

$$\bar{H}_{PS} = \bar{0}; \quad \bar{G}_{PS} \leq \bar{0} \quad (10.1)$$

² Binary variable: 0 means no bleed air is taken from the bleed port

³ This variable takes different values in different mission segments

⁴ W_{TO} is a figure of merit commonly used by the aircraft/aerospace community

$$\text{and } \bar{H}_{ECS} = \bar{0}; \quad \bar{G}_{ECS} \leq \bar{0} \quad (10.2)$$

where the vectors of equality constraints \bar{H} represent the thermodynamic and physical models (weight and volume) for each of the sub-systems. The vectors of inequality constraints \bar{G} represent the physical limits on some of the variables or physical quantities.

TABLE II. ECS DECISION VARIABLES AND CONSTRAINTS

Component	Synthesis / Design Decision Variable		Constraints	
Primary and secondary heat exchangers	L_c	Cold side length (m)	$0.5 < L_c < 0.9$	
	L_h	Hot side length (m)	$0.06 < L_h < 0.9$	
	L_n	Non-flow length (m)	$0.5 < L_n < 0.9$	
Air cycle machine	PR_{cp}	Compressor design PR	$1.8 < PR_{cp} < 3.0$	
	PR_{tb}	Turbine design PR	$PR_{tb} < 12$	
First and second regenerative HXs ⁵	L_c	Cold side length (m)	$0.3 < L_c < 0.5$	
	L_h	Hot side length (m)	$0.15 < L_h < 0.3$	
	L_n	Nonflow length (m)	$0.3 < L_n < 0.5$	
	Reg_1 Reg_2	Existence-nonexistence of regenerative HX in configuration	$Reg_1, Reg_2 = 0, 1$ $Reg_1 + Reg_2 = 1$	
Ram air inlet, outlet	A_1, A_2	Areas of inlet, outlet (cm ²)	$120 < A_1, A_2 < 220$	
Primary and secondary HX fin type: hot and cold sides ^{6,7}	Fin_{hot} Fin_{cold}	Fin No.	Surface designation ⁸	R_{emax}
		1	¼(s)-11.1	8000
		2	1/8-15.2	6000
		3	1/8-13.95	6000
		4	1/8-15.61	6000
		5	1/8-19.86	5000
		6	1/9-22.68	5000
		7	1/9-25.01	4000
		8	1/9-24.12	4000
		9	1/10-27.03	4000
		10	1/10-19.35	4000
Operational Decision Variables				
Pressure regulating valve	PR_{vv}	Pressure setting	$PR_{vv} < 6.0$	
Low pressure bleed port	BP_{low}	Low pressure bleed port ⁹	$BP_{low} = 0, 1$	
High pressure bleed port	BP_{high}	High pressure bleed port ¹⁰	$BP_{high} = 0, 1$	
Splitter	m_{byp}	Bypass air flow rate	$m_{byp} < 0.2 \text{ kg/s}$	
Bleed port	m_{hot}	Hot air flow rate	$m_{hot} < 0.2 \text{ kg/s}$	
Regenerative HX	m_{reg}	Cold air flow rate	$m_{reg} < 0.2 \text{ kg/s}$	
Dependent variables				
Cold and hot sides HXs	Re_c ¹⁰	Reynolds number, cold air side	$Re_c, R_{emax} < 1$	
	Re_h ¹¹	Reynolds number, hot air side	$Re_h, R_{emax} < 1$	
Cabin and avionics	T_{cold} ¹¹	Cooling air temperature	$ T_{cold} - T_{sched} < 3$	
	P_{cold} ¹¹	Cooling air pressure	$P_{cold} = P_{sched}$	
	m_{cold} ¹¹	Cooling air flow rate	$m_{cold} = m_{sched}$	
ACM	W_{cp}, W_{tb} ¹¹	Compressor and turbine work	$W_{cp} = W_{tb}$	

⁵ The cooling air-side of the heat exchanger has 4 passes. The cold and hot sides use fin numbers 4 and 8, respectively. The plate thickness is 0.254 mm.

⁶ Discrete variable.

⁷ The plate thickness is 0.254 mm.

⁸ See Kays and London (1998).

⁹ Binary variable: 0 means no bleed air is taken from the bleed port.

¹⁰ This variable takes different values in different mission segments.

It is important to note that although the minimization of weight is not a thermoeconomic problem, it shares many of its characteristics. For example, the synthesis/design and operation of any given sub-system forces the sub-systems with which it interacts to change their size. In the present problem, that change is reflected in different weights and in a thermoeconomic problem in different costs.

For purposes of defining the optimization problem, it is necessary to subdivide the mission of *Figure 1* into segments (phases or legs). A preliminary analysis reveals that the mission segments and phases of TABLE III are the most critical ones, either because their fuel consumption is significant or the operating conditions are very stringent for the two sub-systems being synthesized / designed.

From TABLE I one sees that the total number of design decision variables for the PS is five. Of the mission legs in TABLE III, six have specified turbine inlet temperature (because military¹¹ or maximum thrust is specified), so that the total number of continuous operational decision variables is nine (T_{it} for the nine remaining legs) The number of binary operational decision variables is two per leg (bleed port selection). Therefore, the total number of independent variables for the PS design optimization problem is forty-four (thirty binary). The total number of constraints is seventy-six.

TABLE III. AAF critical mission segments.

Mission segments		
No.	Name	
1	wup	Warm-up
2	tka	Take-off acceleration
3	tkr	Take-off rotation
4	clac	Climb/accelerate
5	scc	Subsonic cruise climb
6	cap	Combat air patrol
7	acc	Acceleration
8	pen	Penetration
9	ct1	Combat turn 1
10	ct2	Combat turn 2
11	cac	Combat acceleration
12	esc	Escape dash
13	scc ₂	Subsonic cruise climb 2
14	loi	Loiter
15	mm	Maximum Mach number

For the ECS synthesis / design optimization, the number of synthesis / design decision variables is nineteen including two binary (existence or non-existence of either one of the regenerative heat exchangers) and two discrete (type of fin for both sides of the primary and secondary heat exchangers from a set of ten). The operational decision variables include four

continuous variables and two binary (bleed port choice) so that the total (i.e. for the entire mission) number is ninety. Therefore, the ECS synthesis / design optimization problem uses one hundred nine independent variables. The number of constraints is one-hundred and eighty.

Given the nature of the simulation and the number and type of variables and constraints, one can clearly see that one is confronted with a very complex, large-scale mixed integer non-linear optimization problem. The difficulty is exacerbated by the following:

- There is a need to iterate until proper convergence of the take-off weight is achieved.
- The engine simulation tool was not specifically written for optimization purposes. Each time a simulation is run, it is necessary to launch the program and read the necessary software licenses. This difficulty added to the previous item makes the take-off weight calculation (for any given set of values of the independent variables) very expensive computationally. The ECS simulation code does not have this drawback since it was developed in-house.
- The presence of both binary and discrete variables makes it necessary to use a heuristic approach: either a genetic algorithm or a simulated annealing optimization algorithm. There are no general gradient-based methods able to solve this mixed integer non-linear programming (MINLP) problem. However, heuristic algorithms impose a significant time penalty in terms of solution time.

With the comments given above, it becomes clear that *decomposition* is not only advisable but desirable. Quite naturally, two problems, one for the PS and another for the ECS, can be defined. In the presentation that follows, the terminology used is consistent with that of the accompanying paper (Muñoz and von Spakovsky, 2001).

3.1.1 PS design optimization problem definition

The resource used to produce the system-level product (thrust) is fuel. An intermediate product/feedback is the bleed air for the ECS. The ECS in turns has an associated drag penalty, which must be overcome by additional thrust. Other information from the ECS to be used in the PS design is the ECS mass and the bleed port selection. Thus, the PS, i.e. power plant, (and incidentally the overall system) design problem is to

Minimize

$$W_{TO} = w_{str}(W_{TO}) + W_{PS} + W_{ECS} + W_{FUEL} + W_{PPAY} + W_{EPAY} \quad (11)$$

¹¹ Military thrust is defined as the thrust obtained with no afterburning and maximum T_{it}

w.r.t. $\{\bar{X}_{PS}, \bar{Y}_{PS}\}$

subject to the thrust equation (equation (1)) and to the following constraints:

$$W_{ECS} - W_{ECS}^0 = 0 \quad (11.1)$$

$$\dot{m}_{bleed_i} - \dot{m}_{bleed_i}^0 = 0 \quad (11.2)$$

$$BP_{low_i} - BP_{low_i}^0 = 0 \quad (11.3)$$

$$BP_{high_i} - BP_{high_i}^0 = 0 \quad (11.4)$$

Constraints (11.1) through (11.4) indicate that the weight of the ECS, the bleed air flow rate, and the bleed port from which it is taken are set equal to the values indicated with the superscript 0. These values are set externally.

3.1.2 ECS synthesis and design optimization problem definition

Before defining the optimization problem for the ECS, its couplings with the PS in terms of intermediate products/feedbacks must be characterized. To begin with, the only PS product being used directly by the ECS is the bleed air. However, this bleed air and the ECS drag penalty also represent feedbacks to the PS as do the ECS weight and the choice of bleed port for each of the legs. Each translates into excess thrust. In order to represent these couplings in the optimization problem definition, the shadow prices (marginal costs) of these coupling functions (bleed air, ECS drag, and ECS weight) for a given selection of the bleed port at different mission legs must be defined. These costs based on the optimum fuel weight for a given leg i are given by

$$\lambda_{bleed_i} = \frac{\partial W_{FUEL_i}^*}{\partial \dot{m}_{bleed_i}} \quad (12)$$

$$\lambda_{decs_i} = \frac{\partial W_{FUEL_i}^*}{\partial D_{ECS_i}} \quad (13)$$

$$\text{and } \lambda_{wecs_i} = \frac{\partial W_{FUEL_i}^*}{\partial W_{ECS}} \quad (14)$$

where the weight of the fuel at the m_{th} leg is given by

$$\begin{aligned} W_{FUEL_m} &= TSFC_m \cdot T_m \cdot \Delta t_m \\ &= W_{TO} (1 - \pi_m) \prod_{j=1}^{m-1} \pi_j \end{aligned} \quad (15)$$

where, as before, π_m is the ratio of the final to the initial weight for leg m as defined by equation (6). The fuel consumed due to the ECS can then be written as

$$W_{FUEL} = W_{FUEL}^0 + \sum_{i=1}^n \left(\lambda_{bleed_i} \dot{m}_{bleed_i} + \lambda_{decs_i} D_{ECS_i} + \lambda_{wecs_i} W_{ECS} \right) \quad (16)$$

where the reference fuel weight W_{FUEL}^0 has been set to correspond to the case with no bleed air, ECS drag, or weight. It has been assumed in equation (16) that the shadow prices (marginal costs) are constant over the range of bleed, drag, and weight of the ECS.

Equation (16) can be disaggregated even further to account for the additional fuel consumption due to each of the different intermediate feedbacks (i.e., bleed, ECS drag and weight) from the ECS. The resulting fuel consumptions are

$$W_{FUEL_{bleed}} = W_{FUEL}^0 + \sum_{i=1}^n (\lambda_{bleed_i} \dot{m}_{bleed_i}) \quad (17)$$

$$W_{FUEL_{decs}} = W_{FUEL}^0 + \sum_{i=1}^n (\lambda_{decs_i} D_{ECS_i}) \quad (18)$$

$$W_{FUEL_{wecs}} = W_{FUEL}^0 + \sum_{i=1}^n (\lambda_{wecs_i} W_{ECS}) \quad (19)$$

To obtain the impact of these factors on the overall objective function, namely the gross take-off weight, equation (11) is solved (i.e. iterated on W_{TO} until convergence is achieved) with the fuel weight values given by equations (17) to (19). Thus, the increase in the gross take-off weight due to the ECS intermediate feedbacks are given by

$$\Delta W_{TO_{bleed}} = W_{TO}(W_{FUEL_{bleed}}) - W_{TO}(W_{FUEL}^0) \quad (20)$$

$$\Delta W_{TO_{decs}} = W_{TO}(W_{FUEL_{decs}}) - W_{TO}(W_{FUEL}^0) \quad (21)$$

and

$$\Delta W_{TO_{wecs}} = W_{TO}(W_{FUEL_{wecs}}) - W_{TO}(W_{FUEL}^0) \quad (22)$$

Thus far, bleed and drag have been referred to in general terms (see equation (16)) and no mention of what properties should be used to represent them has been made. In the case of bleed air, the options are energy, exergy (or some other thermodynamic property) or air flow rate. Drag can be represented as a force or a form of energy or exergy (i.e. propulsive power loss). The work of Muñoz and von Spakovsky (2000b, 2001) indicates that there is a mathematical advantage to the use of properties that make the shadow prices (marginal costs) monotonic and, ideally, linear. In a different paper, the same authors (Muñoz and von Spakovsky, 2000a) found a linear relationship between fuel consumption and bleed air flow rate as well as

between fuel consumption and drag force. These findings constitute a good choice for the property to represent bleed and drag. In addition, there is an intrinsic practical advantage with the use of these two properties. The engine simulator can be easily adjusted to provide variable air flow rates at the high and low bleed ports. It is also easy to increase or decrease the necessary thrust according to the drag penalty created by the ECS.

One problem arising from the use of bleed air flow rate is the need for “matching” the bleed port temperatures and pressures in both sub-systems for all mission legs. The PS is designed with assumed values for the drag, bleed air flow rate, and weight of the ECS. If the overall system is optimized without decomposition, the values used by the PS and obtained from optimizing the ECS are identical. However, the iterative version of the decomposition approach used (ILGO) makes it necessary in the ECS synthesis/design to use the temperature and pressure of the bleed port obtained from running the PS in the previous iteration. Therefore, it is necessary to check that in addition to flow rate, the bleed thermodynamic conditions are consistent. Although this potentially poses a problem in terms of convergence, we believe that the expected low variability of the bleed port conditions after a few iterations will render this problem insignificant.

With the above comments and taking into account that there is no external resource being used by the ECS, the synthesis/design problem for the ECS is set up as follows:

Minimize

$$\Delta W_{TO_{ECS}} = \Delta W_{TO_{bleed}} + \Delta W_{TO_{decs}} + \Delta W_{TO_{wecs}} \quad (23)$$

w.r.t. $\{\bar{X}_{ECS}, \bar{Y}_{ECS}\}$

subject to the constraints given in TABLE II as well as

$$[P_{bleed}]_{PS} = [P_{bleed}]_{ECS}; [T_{bleed}]_{PS} = [T_{bleed}]_{ECS} \quad (23.1)$$

i.e. the bleed pressures and temperatures must match.

3.2 Fuel consumption problem definition

In addition to using the gross take-off weight as the figure of merit for defining the overall optimization problem, total fuel consumption could be used as well. This optimization problem is defined for the PS as

Minimize

$$W_{FUEL} = w_{fuel}(W_{TO}, \bar{X}_{PS}, \bar{Y}_{PS}, \text{mission}) \quad (24)$$

w.r.t. $\{\bar{X}_{PS}, \bar{Y}_{PS}\}$

subject to the same constraints as in problem (11). It is implicit in the formulation of problem (24) that the fuel consumption over the entire mission is calculated using proper values for the products and feedbacks of the ECS. Note that equation (24) is expressed as a functional relationship since the expression, which defines W_{FUEL} , is too complicated to reproduce here.

For the ECS, the optimization problem is expressed as

Minimize

$$\Delta W_{FUELECS} = \sum_{i=1}^n \left(\lambda_{bleed_i} \dot{m}_{bleed_i} + \lambda_{decs_i} D_{ECS_i} + \lambda_{wecs_i} W_{ECS} \right) \quad (25)$$

w.r.t. $\{\bar{X}_{ECS}, \bar{Y}_{ECS}\}$

subject to the same constraints as in problem (23). In the above equation, n is the number of mission segments.

3.3 Total cost problem definition

The final figure of merit considered in defining the overall optimization problem is total cost. The cost minimization problem for the PS is defined as

Minimize

$$C_T = C_{STR} + C_{PS} + C_{ECS} + C_{FUEL} \quad (26)$$

w.r.t. $\{\bar{X}_{PS}, \bar{Y}_{PS}\}$

subject to the same constraints as in problem (11).

Similarly the cost-based synthesis/design problem for the ECS is

Minimize

$$\Delta C_{TECS} = C_{ECS} + (\Delta C_{FUEL} + \Delta C_{STR} + \Delta C_{PS})_{ECS} \quad (27)$$

w.r.t. $\{\bar{X}_{ECS}, \bar{Y}_{ECS}\}$

subject to the same constraints as in problem (23). ΔC_{TECS} is the increase in the system's total cost due to the ECS, C_{ECS} the capital cost of the ECS, ΔC_{FUEL} the cost of extra fuel due to ECS penalties (bleed air, ram drag, and ECS weight), and ΔC_{STR} and ΔC_{PS} the extra costs of the structures and PS due to the ECS.

4. Solution Approach

One of the options available for solving the optimization problems defined above is the local-global optimization (LGO) decomposition technique presented in Muñoz and von Spakovsky (2000b, 2001). In order to do this, the design of the PS (problem (11)) would need to be carried out for multiple bleed air flow rates, ECS drags and ECS weights, and bleed port selections. This would mean that a number of

optimization runs with respect to the PS design and operational variables would have to be solved for innumerable combinations of values of the constraints (11.1) to (11.4). The same number of optimizations would have to be done for the ECS. The results would then be used to generate the optimum response surface (ORS) of the system, which for the first figure of merit would be in the WTO vs. ECS drag, bleed, and weight domain. If this off-line version of the method (OL-LGO; see Muñoz and von Spakovsky (2000b, 2001)) were used, the results would have to be stored for later use in the system-level optimization problem for the PS and ECS combined. The latter problem involves finding the combination of bleed air, ECS drag, and weight that minimizes the system-level objective function.

From a practical point of view, there are a number of difficulties associated with the implementation of the OL-LGO technique in its general form for this case. These difficulties are summarized as follows:

- The calculation of the take-off gross weight involves “flying” the engine on paper over the entire mission to obtain the fuel consumption. The process is repeated a number of times until convergence on the take-off weight is achieved. The resulting W_{TO} value can then be sent to the optimizer for analysis.
- The process described in the previous item requires different computer codes. First, there is a computer program that calculates the necessary thrust for each of the mission legs by solving the differential equation (7) and the thrust and fuel consumption and weight equations (fly dynamics code). The thermodynamic engine simulation follows. This step is particularly slow due to the fact that the engine performance code in use is not ‘persistent’, i.e. it is necessary to launch the program every time the engine is ‘flown’ over the mission. The thrust obtained from the engine simulator is adjusted by a different computer code to account for inlet and nozzle losses, as indicated by Muñoz and von Spakovsky (2000c). Some of the outputs of the thermodynamic simulation added to aerodynamic, material and other design variables are used by WATE (NASA’s engine weight code) to calculate the weight of the engine. The final step is the post-processing of all of the codes’ results. The entire process just described makes the simulation very expensive computationally. For reference, the calculation of a single value for the take-off gross weight takes on average about 55 seconds on a current PC workstation, a duration which can be prohibitive for large-scale optimization.

The previous discussion points to the need for the iterative version of the LGO technique,

i.e. ILGO, as presented in Muñoz and von Spakovsky (2000b, 2001). Of the two versions of ILGO presented in these references, version A requires that both the PS and ECS be designed for arbitrary values of the intermediate products and feedbacks (i.e. ECS bleed, drag, and weight). Such a constraint is easy to meet in the PS design. However, the ECS synthesis/design would unnecessarily be constrained by this requirement. In fact, arbitrary combinations of the coupling functions between the PS and ECS may not necessarily lead to feasible solutions for the ECS. Therefore, version B of ILGO, which does not have these shortcomings, is used for the ECS synthesis / design optimization while version A is retained for the PS.

The implementation of ILGO requires the following steps:

1. The first step is to design the PS (i.e. begin solving optimization problem (11)) for an initial estimate of the necessary amount of bleed air and ECS drag and weight. Since no information about the ECS exists at this stage of the design process, estimates are used based on Muñoz and von Spakovsky (2000a). Thus, the initial amount of bleed air is estimated as 120% of the amount of air required to cool the load (cabin and avionics). The ECS drag is initially estimated at 1200 N for each of the legs. An initial estimate for the ECS weight is 410 kg (900 lbm). To begin with, it is assumed that the bleed air is taken from the high-pressure bleed port at all points of the mission. Once the bleed port has been chosen and the amount of bleed air and the ECS drag and weight are fixed, the number of independent variables is effectively reduced from 44 to 14, none of which is an integer.

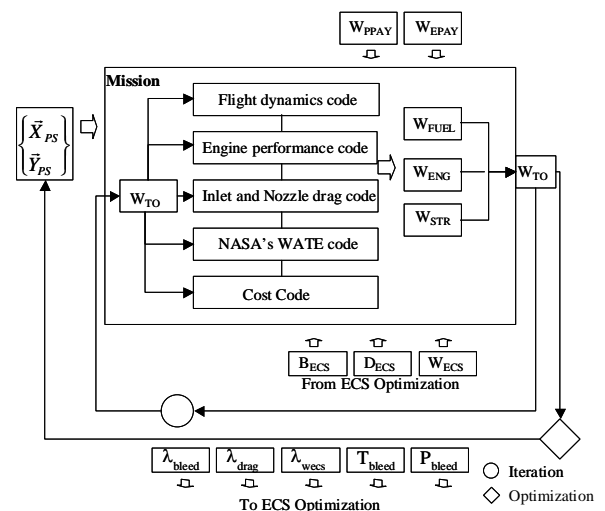


Figure 4. PS modeling/optimization procedure.

- After completing the PS design, the bleed port thermodynamic conditions are calculated at all operating conditions (mission segments). The fuel-based shadow prices for each of the mission legs are calculated as well in this step. The entire modeling/optimization process for the PS design optimization is depicted in *Figure 4*.
- The bleed and pressure values for each of the mission legs along with the shadow prices are used to carry out the synthesis / design optimization of the ECS (problem (23)). Based on the previous work of Muñoz and von Spakovsky (2000a), the shadow prices are assumed constant over the synthesis/design space. This assumption is equivalent to saying that the response surface is in fact a hyper-plane. With the previous supposition, the coupling functions are allowed to take arbitrarily large or small numbers. To begin the solution of problem (23), the bleed pressure and temperature maps presented by Muñoz and von Spakovsky (1999) are used. The total number of variables is 109. Given the large number of variables and the fact that 4 of them are integer for the ECS problem, time decomposition is used in the manner described in Muñoz and von Spakovsky (2000b, 2001). The work of Muñoz and von Spakovsky (1999) shows that the most demanding operating condition for the ECS corresponds to the mission segment with high altitude and subsonic speed. This point is critical because of a combination of relatively low bleed pressures, high cooling temperatures, and low ram air availability. Thus, the selected synthesis/design or reference condition corresponds to the second subsonic cruise climb leg of TABLE III.

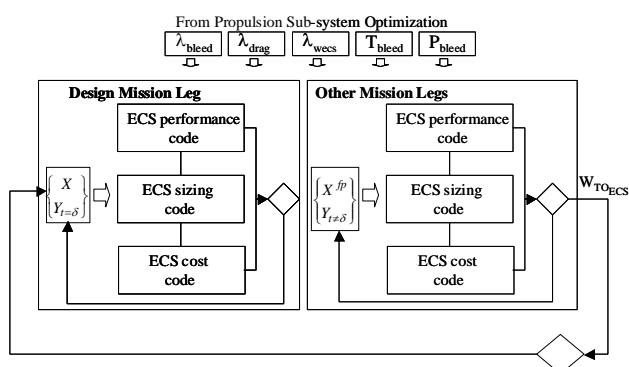


Figure 5. ECS decomposed optimization approach.

- The second subsonic cruise climb leg is used to obtain a set of the most promising solutions. Each of these (typically 5) provides constant values for the ECS

synthesis/design decision variables, which are then used in the off-design optimization. At the operational-level, fourteen problems are resolved each with respect to the operational decision variables for each leg. The optimization procedure for the ECS is shown in *Figure 5*.

- Once completed, the ECS synthesis/design provides updated values for the intermediate products and feedbacks of the ECS (i.e. the coupling functions). These values are used in step 1 to redesign the PS. The iterative process continues until no improvement in the overall objective function is observed.
- An additional consideration is that the bleed pressure and temperature for the optimized PS should be equal to those used in the optimization of the ECS. The final match between bleed air properties is to be verified.

The procedure described above is the same regardless of whether the objective function is the total gross take-off weight, the fuel consumed to carryout the mission, or the total cost.

All of the optimization problems are solved using the commercial optimization package iSIGHT (1999). First, a Genetic Algorithm (GA) is used in order to effectively deal with the mixed integer variables and possible local minima problems in each of the unit (sub-system) optimizations. Each GA optimization run has a minimum population size equal to three times the number of variables with a minimum of 50. The minimum number of iterations for the GA is set to 100 and 1000 times the population size for the PS and ECS optimization problems, respectively. Using the GA, the convergence criterion for the calculation of the take-off gross weight is set at 0.2 %. This means that the value of W_{TO} sent to the optimization algorithms has an error of approx. ± 200 N. Once the top two or three solutions have been obtained with the GA, a gradient-based algorithm (Method of Feasible Directions) is used to narrow down the best solutions. In this case, the convergence criterion in the take-off gross weight calculation is set at 0.1 %.

5. Results

All three figures of merit were used to optimize the synthesis/design of the PS / ECS system, and the results show that total fuel consumption for the mission and system total cost are linear with respect to gross take-off weight (Muñoz and von Spakovsky, 2000c; Muñoz, 2000). Since the optimum solution is, thus, independent of the objective function used, only the results for the gross take-off weight minimization problem are reported here. An optimum value for the gross take-off weight was

found in 4 iterations using ILGO. A match between the bleed properties used in the ECS and PS optimization problems was verified as reported by Muñoz and von Spakovsky (2000c)

Figure 6 shows the evolution of the gross take-off weight and the weights of the PS and ECS for each iteration. It is clearly evident that in each iteration some improvement was achieved in the objective function (gross take-off weight) and the weights of both sub-systems. The flat behavior of W_{TO} for the last two iterations indicates that the overall iterative optimization scheme converged, i.e. no improvement is achieved after iteration 4. This observation was verified by running the problem a fifth time with no observable change in the independent variables or the objective function.

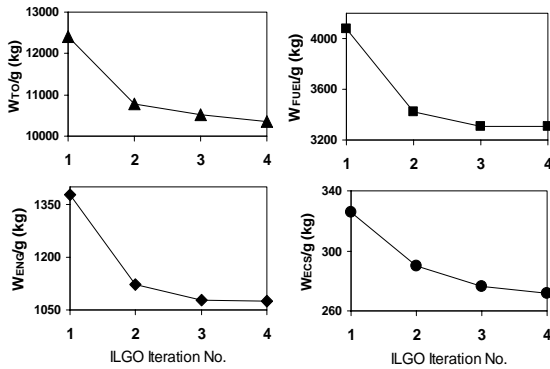


Figure 6. Evolution of the gross take-off weight, fuel, and ECS and PS weights at different points of the ILGO approach.

The change of selected independent variables for both the PS and ECS for the different optimization runs is shown in Figure 7. The evolution of the ram air scoop inlets and core dimensions of the primary heat exchanger are shown as well as the fan bypass and pressure ratio, the high pressure compressor's and low and high pressure turbines' design pressure ratios. All of the variables have been non-dimensionalized by dividing them by the minimum allowable value found in TABLE I and II.

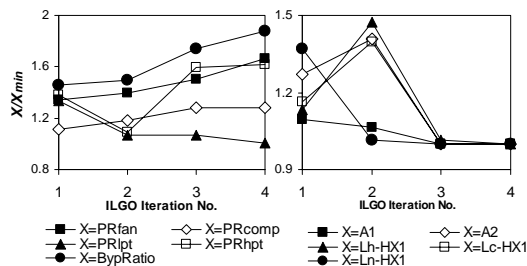


Figure 7. Change of select independent variables for the ECS and PS synthesis/design as the ILGO scheme progressed.

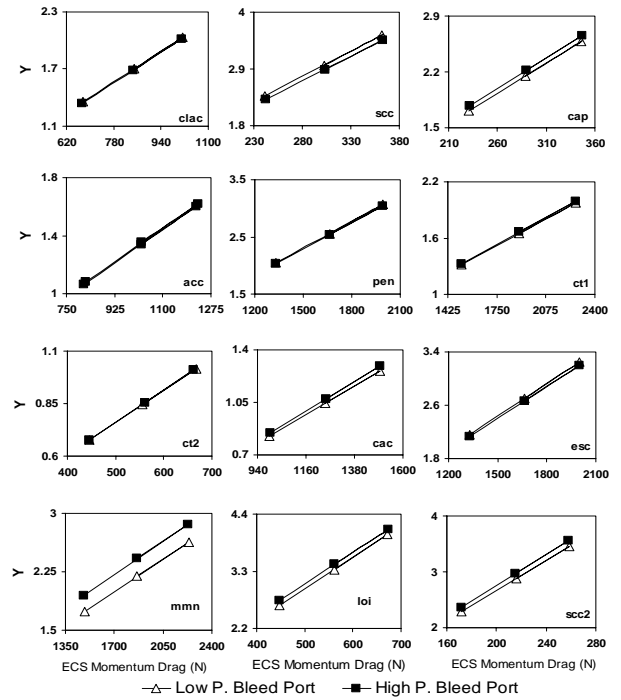


Figure 8a. Incremental fuel consumption due to ECS momentum drag at different mission legs. The slopes of the curves are the drag shadow prices based on fuel.

$$Y \equiv \frac{W_{FUEL}(\dot{m}_{bleed_i}, D_{ECS}) - W_{FUEL}(bleed, 0)}{W_{FUEL}(bleed, 0)} \times 100$$

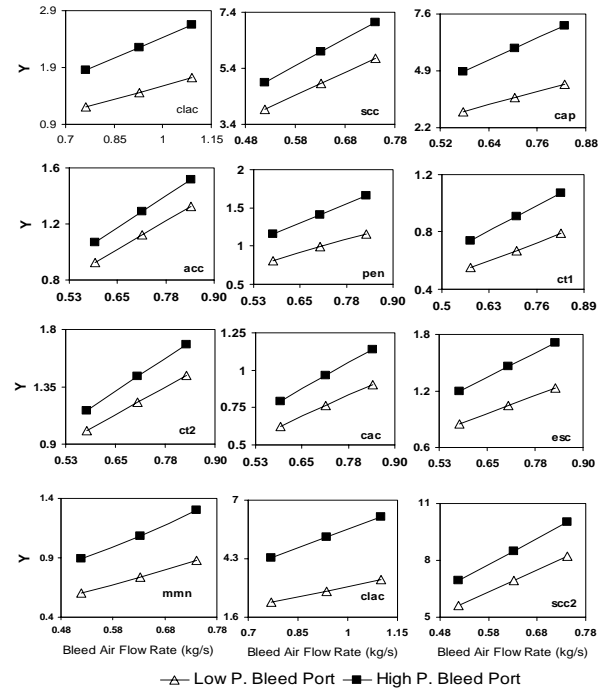


Figure 8b. Incremental Fuel consumption due to ECS bleed air extraction at different mission legs. The slopes of the curves are the bleed air shadow price based on fuel.

$$Y \equiv \frac{W_{FUEL}(\dot{m}_{bleed_i}, D_{ECS}) - W_{FUEL}(0, D_{ECS})}{W_{FUEL}(0, D_{ECS})} \times 100$$

The shadow prices at the optimum for selected mission legs are given in *Figure 8*. The linear behavior of the shadow prices for both design and off-design conditions is clearly evident. This behavior is observed even though no energy or exergy quantities were used. The fact that the shadow prices represented by the slope of the curves in *Figure 8* are constant most likely helped the relatively fast overall convergence of the ILGO scheme used. In Muñoz and von Spakovsky (2000b, 2001), it was theorized that constant shadow prices would lead to the final solution in only one iteration (i.e. effectively “thermoeconomic isolation” Frangopoulos and Evans, 1984; von Spakovsky and Evans, 1993). This was not the case in this application, primarily due to the initial mismatch between bleed conditions used in the ECS optimization and those obtained from running the PS.

TABLE IV. PS AND ECS OPTIMUM SYNTHESIS AND DESIGN VARIABLES

L_h (Prim HX)	0.500	α	0.563
L_c (Prim HX)	0.060	PR _{fan}	4.997
L_n (Prim HX)	0.500	PR _{hpc}	5.140
L_h (Sec. HX)	0.500	PR _{hpt}	2.907
L_c (Sec. HX)	0.060	PR _{lpt}	1.814
L_n (Sec. HX)	0.508	PR _{cp}	2.60
L_c (Reg. HX)	0.300	PR _{tb}	8.56
L_c (Reg. HX)	0.150	Fin _{hot}	4
L_n (Reg. HX)	0.300	Fin _{cold}	4
A ₁	120.0	Reg ₁	0
A ₂	120.0		

TABLE V. PS AND ECS OPTIMUM OPERATIONAL VARIABLE VALUES

Leg	PR _{vv}	m _{creg}	m _{byp}	m _{hot}	BP _{low} ¹²	BP _{high}	T _{it}
Tkr	1.406	0.017	0.000	0.000	0	1	1778
Tka	2.193	0.035	0.200	0.000	0	1	1778
Wup	1.845	0.001	0.063	0.000	0	1	1778
Clac	3.440	0.056	0.101	0.000	1	0	1778
Sec ₁	2.459	0.104	0.002	0.000	1	0	1355
Cap	1.380	0.200	0.002	0.000	0	1	1090
Acc	4.029	0.101	0.001	0.044	1	0	1778
Pen	5.564	0.062	0.001	0.000	1	0	1588
ct1	6.000	0.069	0.016	0.000	1	0	1778
ct2	4.229	0.087	0.032	0.000	1	0	1778
Cac	5.885	0.058	0.016	0.000	1	0	1778
Esc	5.287	0.086	0.032	0.000	1	0	1574
Mmn	4.229	0.137	0.024	0.000	1	0	1636
Sec ₂	1.463	0.088	0.000	0.000	1	0	1275
Loi	2.115	0.015	0.048	0.000	1	0	1113

¹² This variable is common to the ECS and PS optimization problems

The shadow prices are indicative of the relative importance of the product going from the PS to the ECS and the feedback coming from the ECS (i.e. the coupling functions). A first order approximation using the allowable ranges for the ECS independent variables of TABLE II reveals that the variability of bleed air flow rate, ECS drag and weight are approximately 0.75 ± 0.2 kg/s, 350 ± 300 N and 700 ± 300 kg, respectively. With these values and the shadow prices of *Figure 9*, one can readily conclude that the effect of the ECS weight is significantly higher than that of the bleed air flow rate and momentum drag. Thus, the optimum ECS solution is expected to have the smallest possible weight. The fact that all of the shadow prices have positive values indicates that a solution with lower bleed and drag will be preferred for a given value of ECS weight as well.

The shadow prices show that weight is the most important of the intermediate products and feedbacks going to and coming from the ECS. TABLE VI indicates that the heat exchangers make the biggest contribution to weight among the components participating in the optimization. With these two observations in mind, it comes as no surprise that the optimum solution found for the ECS corresponds to the synthesis/design with the lowest possible heat exchanger core dimensions. Additionally, since ram air has an incremental impact on fuel consumption (and hence on W_{TO}) due to the extra thrust needed (via momentum drag) and mass required (that of the ram air inlet and exit), the minimum ram air inlet areas are also expected.

Finally, the optimizer found an optimum solution for the PS with the highest possible turbine inlet temperatures. Again, this is an expected result due to the fact that it is much more efficient to burn fuel in the combustor than in the afterburner.

TABLE VI. ECS AND PS OPTIMUM RESULTS.

$\Delta W_{TOECS}/g$ (kg)	852	W_{TO}/g (kg)	10364
$\Delta W_{FUELECS}/g$	551	W_{FUEL}/g	3308
$\Delta W_{FUELbleed}/g$	79	W_{STR}/g	4526
$\Delta W_{FUELdecs}/g$	52	W_{ENG}/g	1075
$\Delta W_{FUELwecs}/g$	420	Fan	229
W_{ECS}/g ¹³	272	Hpc	121
Prim HX	24	Hpt	142
Sec. HX	24	Lpt	243
Reg. HX	11	Noz	52
ACM	12	Other	288
Ram Inlets	11	C_{ECS} ¹⁴	541
Ram exits	9	C_{FUEL}	778
Ducting ¹⁵	129	C_{STR}	14140
Other ¹⁵	17	C_{PS}	5642

¹³ Includes 15% additional mass for packaging and installation. All of the component weights include accessories.

¹⁴ All costs in thousands of 1999 US dollars.

¹⁵ Not participating in the optimization

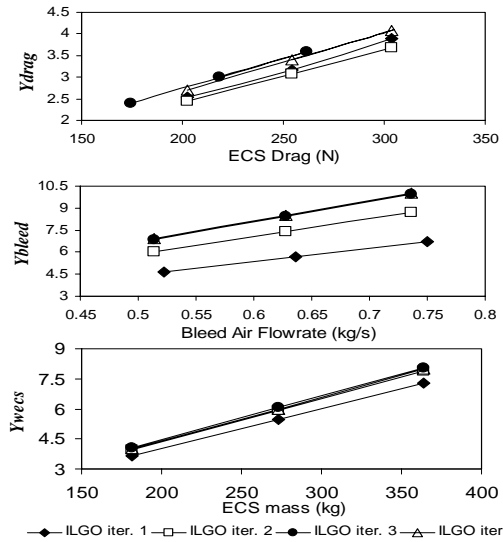


Figure 9. ECS drag, mass and bleed air shadow prices at the design point (scc_2) for different iterations of the ILGO scheme. The shadow prices are the slopes of the curves. The fact that the shadow prices are constant indicate that the ORS is a hyper-plane.

$$Y_{drag} \equiv \frac{W_{FUEL}(\dot{m}_{bleed_i}, D_{ECS}, W_{ECS}) - W_{FUEL}(\dot{m}_{bleed_i}, 0, W_{ECS})}{W_{FUEL}(bleed, 0, W_{ECS})} \times 100$$

$$Y_{bleed} \equiv \frac{W_{FUEL}(\dot{m}_{bleed_i}, D_{ECS}, W_{ECS}) - W_{FUEL}(\dot{m}_{bleed_i}, 0, W_{ECS})}{W_{FUEL}(bleed, 0, W_{ECS})} \times 100$$

$$Y_{wecs} \equiv \frac{W_{FUEL}(\dot{m}_{bleed_i}, D_{ECS}, W_{ECS}) - W_{FUEL}(\dot{m}_{bleed_i}, D_{ECS}, 0)}{W_{FUEL}(bleed, D_{ECS}, 0)} \times 100$$

6. Comments / Discussion

6.1. The global optimality of the solution

In order to study the global characteristics of the ILGO approach from a purely numerical standpoint¹⁶, the solution results for the ILGO approach were compared to those obtained without decomposition, i.e. when the optimization problem is treated as a whole. The objective function used was gross take-off weight. Obviously the number of independent variables had to be reduced to facilitate the solution of the system-level problem when taken in its entirety. Thus, the problem was solved with and without decomposition using the reduced variable set.

The PS design variables chosen were fan bypass ratio and fan and high pressure compressor pressure ratio. The low and high pressure turbine design pressure ratios were set at 2.0 and 2.2 respectively. The operational variables are given in TABLE I with one exception: the bleed port from which air for the ECS is taken at different mission segments was fixed at the values given in TABLE V.

¹⁶ Note that the theoretical or mathematical foundations for global optimality were presented in Muñoz and von Spakovsky (2000b).

The number of ECS synthesis/design and operational variables was also reduced. All of the integer variables were fixed by selecting the second regenerative heat exchanger in Figure 3 and choosing fins No. 5 and 7 for the cold and hot sides of the primary and secondary heat exchangers. The ACM compressor design pressure ratio was chosen to be 2.6. The core dimensions of the regenerative heat exchanger were fixed at 0.4, 0.2 and 0.4 m for the cold, hot and non-flow sides, respectively. The only ECS operational variables used were the valve pressure setting and the bypass air flow rate. This selection of operational independent variables fixed the amount of bleed air taken from the main engine compressor (the amount of cooling air required in the cabin and avionics is a function of altitude and Mach number). The regenerative heat exchanger's cold air flow rates were set at 0.05 kg/s and no hot air was allowed.

The number of iterations required for ILGO to obtain a solution for the reduced problem was again 4. The final results with and without decomposition are given in TABLES VII to IV. Quite clearly, the solutions obtained from both methods are basically identical. The decomposed solution is well within 0.5 % of the solution obtained without decomposing the problem. It is important to note that the solution without decomposition took more than ten thousand iterations to converge. Thus the optimization took six and a half days running on two PC workstations, each with dual state of the art processors running in parallel. The time for the decomposed optimization was about two and a half days. Obviously, the decomposition approach required a lot more human intervention, which in fact mirrors the discipline-oriented nature of existing engineering practice and, thus, conceptually derives another advantage in terms of implementation for the ILGO approach over that without decomposition.

The behavior of the shadow prices for this simplified problem were similar to those shown in Figures 8 and 9. The fact that the shadow prices are of the same sign (in fact are approximately constant) for all iterations is believed to be a major contributing factor to the global convergence of the ILGO approach as shown in the accompanying paper by Muñoz and von Spakovsky (2001). These conditions are believed to be indicative of the convexity of the restricted optimum values of the overall objective function with respect to the coupling functions, which in this case are bleed air and ECS drag and weight.

TABLE VII. COMPARISON OF RESULTS FOR THE OVERALL SYNTHESIS/DESIGN OPTIMIZATION PROBLEM WITH AND WITHOUT DECOMPOSITION.

	Decomposition (ILGO)	No Decomposition
L_h (Prim HX)	0.500	0.500
L_c (Prim HX)	0.060	0.060
L_n (Prim HX)	0.500	0.500
L_h (Sec. HX)	0.500	0.501
L_c (Sec. HX)	0.060	0.060
L_n (Sec. HX)	0.500	0.500
A_1	120	121
A_2	120	120
PR_{th}	5.08	5.21
α	0.398	0.393
PR_{fan}	4.50	4.45
PR_{hpc}	5.66	5.67

TABLE VIII. ECS AND PS OPTIMUM OPERATIONAL VARIABLES (CASE WITHOUT DECOMPOSITION)

Leg	PR_{vv}	m_{bvp}	T_{it}
tkr	1.643	0.060	1778
tka	1.736	0.039	1778
wup	1.715	0.008	1778
clac	2.572	0.030	1778
scc1	2.016	0.000	1341
cap	1.978	0.001	1056
acc	5.545	0.000	1778
pen	2.016	0.000	1528
ct1	2.426	0.000	1778
ct2	1.819	0.000	1778
cac	5.631	0.000	1778
esc	2.616	0.000	1517
mmn	3.270	0.000	1600
scc2	1.153	0.194	1354
loi	1.431	0.200	1005

TABLE IX. ECS AND PS OPTIMUM RESULTS.

	Decomposition (ILGO)	Without Decomposition
W_{TO}	11526	11466
W_{FUEL}	3776	3734
W_{ENG}	1295	1299
W_{ECS}	314	314

In order to verify some of the theoretical foundations for the ILGO approach and the reasons for its global convergence, the Optimum Response Surface for the reduced problem was constructed using twenty uniformly distributed points across the design space. A cubic interpolation routine was used to obtain a smooth surface of the gross take-off weight versus ECS drag (at the design point) and weight. The resulting surface plot, i.e. the ORS, is shown in Figure 10.

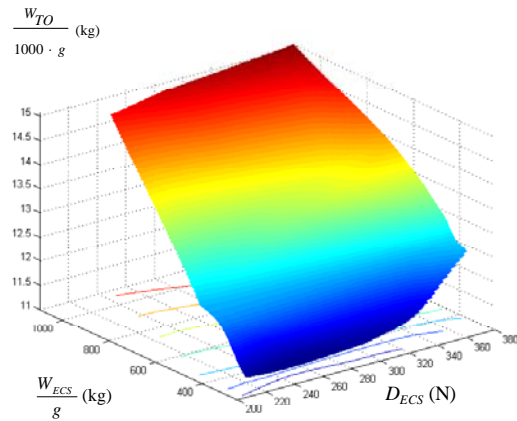


Figure 10. Optimum response surface for the restricted take-off gross weight minimization problem.

Figure 10 has several interesting features. The first is that the design space in ECS drag and weight is not only convex but shows an almost flat behavior, typical of a linear system¹⁷. This is to be expected since the partial derivatives of the objective function (W_{TO}) with respect to the intermediate products and feedbacks (the shadow prices) are basically constant throughout the entire optimization process. The second important feature is that Figure 10 shows the great impact of the ECS weight on the objective function. The best solution is the one with the lowest possible weight. This, again, is to be expected given the large value of the weight's shadow price when compared to that of bleed and drag. This may explain the relatively minor effect of ECS drag, although there is clearly a tendency to have smaller W_{TO} values with low drag for a given weight. The effect of drag is not completely independent of weight, however, since ECS drag implies the need for a bigger and, therefore, heavier ram air scoop inlet. Furthermore, a larger ram air duct leads to increased ram air flow and possibly larger heat exchangers.

7. Conclusions

An application of the iterative version of the Local-Global Optimization decomposition algorithm (ILGO) developed in Muñoz and von Spakovsky (2000b, 2001) was demonstrated. ILGO was specifically developed keeping in mind a number of practical considerations. In particular, the ILGO approach for synthesis / design optimization was set up trying to mimic

¹⁷ It must be stressed that the objective function is linear with respect to the intermediate products and feedbacks (coupling functions) and not with respect to the individual sub-system independent variables. With respect to the latter it is, in fact, highly non-linear.

and enhance current engineering practice such that:

- The analysis and optimization of each unit (sub-system) is modular and divided into clearly separated tasks. In industry, these tasks are performed by specialized groups.
- The two unit optimizations were carried out concurrently.
- Human intervention was supported.
- Advanced, high-fidelity tools for the system and load simulations were used.
- Sub-system optimizations were kept at a minimum possible.
- In each iteration of ILGO, improvements in the objective functions were achieved. In the event of a halt to the synthesis / design process due to extraneous reasons, an improved synthesis / design over that of the starting or reference synthesis / design would already have been achieved.

In addition to the above practical features, a number of theoretical issues were addressed. First, the MINLP for the entire system was solved and the global convergence of the method was verified. Additionally, fast convergence was achieved. Both of these results are due to the high linearity of the ORS. The latter finding was initially hypothesized based on the observed constant behavior of the shadow prices and later graphically verified.

Finally, it is important to note that the linearity mentioned above was obtained by representing the coupling functions with properties that were not exergy or even energy based. The properties used resulted not only in linear behavior but also eased calculation of the shadow prices and in the future may provide the possibility of linking the sub-systems synthesized / designed to non-energy based sub-system syntheses / designs (e.g., the aircraft structure, etc).

Acknowledgements

This work was conducted under the sponsorship of the U.S. Air Force Office of Scientific Research

Thanks are due to Walter O'Brien of Virginia Tech for providing his expertise in the selection of aerodynamic and other design variables for the propulsion sub-system. Tom Cunningham helped a great deal in putting the engine model together. Richard Smith and Roland Watts of AFRL helped in the painstaking labor of gathering information for constructing the ECS models. Many thanks are due to Mike Tong of NASA Lewis Research Center for his help with the implementation of WATE.

Nomenclature

A	Area
AAF	Air-to-Air Fighter
bleed	ECS bleed
BP	Bleed port
C	Monetary cost
C_D	Drag coefficient
C_{D0}	Drag coefficient at zero lift
C_L	Lift coefficient
D	Drag
ECS	Environmental Control Sub-System
fp	Feasible and promising
g	Acceleration of gravity
\bar{G}	Vector of inequality constraints
h	Altitude
HPC hpc	High pressure compressor
HPT hpt	High pressure turbine
HX	Heat exchanger
\bar{H}	Vector of equality constraints
K	Constant
LPT	Low pressure turbine
lpt	Low pressure turbine
M	Mach number
mil	Military
N	Number of turns
n	Load factor
PR	Pressure ratio
PS	Propulsion Sub-system
R	Additional or "parasitic" drag
Re	Reynolds number
RFP	Request for proposal
S	Wing planform area
SL	Sea level
STR	Structures Sub-system
t	Time
T	"Installed" thrust
V	Velocity
WATE	Weight Analysis of Turbine Engines
\bar{X}	Vector of design variables
\bar{Y}	Vector of operational variables

Superscripts

o	Reference, initial value
*	Restricted Optimum
**	Unrestricted optimum

Subscripts

o	Reference, initial value
0	Ambient
decs	ECS drag
wecs	ECS weight
SL	Sea level

Greek

α	Thrust fraction, engine bypass ratio
β	Weight fraction
γ	Specific heat ratio
λ	Shadow price, vector of shadow prices

Λ	Shadow price, vector of shadow prices
π	Leg weight ratio
ϕ	Inlet and nozzle drag coefficients

References

Evans, R.B., and von Spakovsky, M.R., 1993, "Engineering Functional Analysis (Part II)," *Journal of Energy Resources Technology*, ASME, Vol. 115, No. 2, N.Y., June.

Frangopoulos, C.A., Evans R.B., 1984, "Thermoeconomic Isolation and Optimization of Thermal System Components," *Second Law Aspects of Thermal Design*. HTD Vol. 33, ASME, N.Y., N.Y., August.

iSIGHT version 5 Designer's Guide, 1999, Engineous Software Inc., Morrisville, N.C.

Jane's All the World's Aircraft 1999-2000, 1999, Jane's Information Group, Coudson, UK

Kays, W.M. and London, A.L., 1998, *Compact Heat Exchangers*, Krieger Publishing Company, Malabar, FL.

Mattingly, J.D., Heiser, W.H. and Daley, D.H., 1987, *Aircraft Engine Design*, AIAA Education Series, New York, New York.

Muñoz J. R., von Spakovsky M.R., 1999, *A Second Law Based Integrated Thermoeconomic Modeling and Optimization Strategy for Aircraft / Aerospace Energy System Synthesis and Design (Phase I – Final Report)*, final report, Air Force Office of Scientific Research, New Vista Program, December.

Muñoz, J.R., 2000, "Optimization Strategies for the Synthesis / Design of Highly Coupled, Highly Dynamic Energy Systems," Ph.D.

Dissertation, Virginia Polytechnic Institute and State University, Blacksburg, VA.

Muñoz, J.R., von Spakovsky, M.R., 2000a, "An Integrated Thermoeconomic Modeling and Optimization Strategy for Aircraft / Aerospace Energy System Design", *Efficiency, Costs, Optimization, Simulation and Environmental Aspects of Energy Systems (ECOS'00)*, Twente University, ASME, Netherlands, July 5-7.

Muñoz, J.R., von Spakovsky, M.R., 2000b, "The Use of Decomposition for the Large Scale Synthesis / Design Optimization of Highly Coupled, Highly Dynamic Energy Systems: Part I - Theory," 2000 ASME International Mechanical Engineering Congress and Exposition, Orlando, FL, Nov 5-10.

Muñoz, J.R., von Spakovsky, M.R., 2000c, "The Use of Decomposition for the Large Scale Synthesis/ Design Optimization of Highly Coupled, Highly Dynamic Energy Systems: Part II - Application," 2000 ASME International Mechanical Engineering Congress and Exposition, Orlando, FL, Nov 5-10.

Muñoz, J.R., von Spakovsky, M.R., 2001, "A Decomposition Approach for the Large Scale Synthesis / Design Optimization of Highly Coupled, Highly Dynamic Energy Systems" *International Journal of Applied Thermodynamics*, March, Vol. 4, No. 1.

Nicolai, L., 1975, *Fundamentals of Aircraft Design*, published by the author.

SAE Aerospace Applied Thermodynamics Manual, 1969, Society of Automotive Engineers, New York.

WATE User's Guide, 1999, NASA Glenn Research Center.